World Applied Sciences Journal 32 (3): 492-504, 2014
ISSN 1818-4952

DOI: 10.5829/idosi.wasj.2014.32.03.389

Observations of Ice Crystals in Cirrus Clouds over Central Thailand

[1]Pakdee Chantraket, [2]Sukrit Kirtsaeng and [3]Supap Kirtsaeng

[1]Department of Royal Rain-making and Agricultural Aviation, Bangkok, Thailand
[2]Meteorological Development Bureau, Thai Meteorological Department, Bangkok, Thailand
[3]Department of Mathematics, Faculty of Science, Silpakorn University, Nakhon Pathom, Thailand

Abstract: Cirrus clouds are generally one of the most occurring cloud types in Thailand and worldwide and play a considerable role in the global heat balance. The knowledge of their information about the habits of microphysical properties is essential for parameterization of particle habits in radiation transfer, weather and climate modeling and in remote sensing retrievals. The state-of-science airborne instrumentation of department of royal rain-making and agricultural aviation (DRRAA) was used to measure the shape and size distribution of cloud particles in case of tropical cirrus. The observation was carried out on 7 September 2011 over three provinces of central Thailand. Four samples of cirrus clouds totaling to 54.2 km of cloud penetration. The samples consist of two cirrostratus (Cs) and two Cirrus (Ci) with temperature between -8°C and 21°C at four different altitudes from 6 km to 10 km. Particle number size distribution (PNSD) between 0.47 µm to 19,200 µm were also constructed with combining measurements from the fast-forward scattering spectrometer probe (Fast-FSSP), two dimensional spectrometer (2-DS) and high volume precipitation spectrometer (HVPS). Images of ice crystals were measured with cloud particle imager (CPI). It was found that the PNSD in Cs clouds clearly exhibit continuously wider spectra with higher total number concentration than Ci clouds. Conversely, Ci clouds contain larger particle diameters, with dominated size around 300 to 500 µm, comparing to particles in Cs clouds which is approximately 10 µm. CPI was used to capture 31,233 images of ice crystals. The analysis shows average maximum aspect ratio (AR) of all sampled cirrus cloud particles ranging from 4.9 to 11. The Cs clouds evidently illustrate a larger AR than the Ci clouds. The proportion of spherical particles in cirrus clouds was found to be approximately 8.45%. Moreover, the study shows that the ratio of spheroids and ice particles in both cirrus types tends to be steady as the temperature cool down beyond -16°C. The analysis of particle sizes and behaviors showed that the cirrus clouds are essentially formed from irregular ice crystals and the pristine ice crystals are rare. Also, the irregular shape particles are evenly distributed in all size categories and usually trend to be a small ice particles of approximately 90 µm.

Key words: Central Thailand · Cirrus clouds · Number concentration · Particle number size distribution (PNSD) · Aspect ratio · Roundness · Ice crystals

INTRODUCTION

Cirrus clouds are designated as high clouds formed in high atmosphere. They are further categorized as cirrus (Ci), cirrostratus (Cs) and cirrocumulus (Cc) clouds. In midlatitudes, they have been conventionally classified as clouds with base heights above about 6 km. In the tropics, cirrus clouds are related to deep cumulus outflows associated with the convective activity with frequency of occurrence higher than 70 % [1]. Cirrus clouds are one of the most commonly occurring cloud types, both in Thailand and globally. They play an important role in the global heat balance and knowledge of their altitude and microphysical properties are essential to climate modeling [2]. Because of their high location in the atmosphere, direct observation of the composition and structure of cirrus is difficult and requires a highflying aircraft platform.

Corresponding Author: Supap Kirtsaeng, Department of Mathematics, Silpakorn University, Nakhon Pathom 73000, Thailand.

Nowadays, the comprehensive information about cirrus composition became available as a result of the development of several airborne instruments. In addition, the advancement of cloud particles instrumental technology has provided the improvement of research tool to sample their particle shapes and size distribution. These instruments included imaging optical probes using a laser beam such as FSSP, 2-DS, HVPS and etc. and high resolution microphotographs such as CPI. EUCREX project [3] which studied clouds in midlatitude, for instance, used 2D-C (Two dimension cloud particle imaging probe) and 2D-P (Two Dimensional Optical Array Precipitation Probe) probes to collect the microphysical data in cirrus clouds over Scotland. The tropical experiments of CRYSTAL-FACE project [4-7] is a measurement campaign using 2D-C, HVPS and CPI designed to investigate tropical cirrus cloud physical properties and formation processes over Florida, USA. Additionally, CEPEX [8-12] was conducted over Pacific Ocean, a Learjet aircraft equipped with 2D-C and 2P-P probes were used to measure the vertical and horizontal structure of cirrus microphysical properties.

For this reason, the perceptions of the climatic effect of cirrus clouds must begin with an in depth understanding of their microscopic composition and associated radiative properties. The ice crystal size and shape distributions are fundamental cirrus parameters that determine the relative strength of the so-called solar albedo (reflection of sunlight) and infrared greenhouse (trapping of thermal radiation) effects, which are essential components in the discussion of cirrus clouds and climate. The results of this study will not only improve our knowledge of the ice crystals in cirrus cloud using research aircraft measurement over Thailand but also provide the comprehension for further study on impacts of cirrus cloud formation processes and the radiative transfer properties of cloud fields in Thailand as well.

The purpose of this study is to investigate the results of a detailed study of ice particles in cirrus clouds including measurements on cirrostratus (Cs) and Cirrus (Ci) clouds obtained in central part of Thailand. The state-of-science airborne instrumentation of DRRAA was used to measure the shape and size distribution of cloud particles in case of tropical cirrus using Fast-FSSP [13], 2-DS and HVPS probes. However, the physical diameter of the crystals cannot be obtained directly from cloud and precipitation probes due to their much more complex particle types and shapes comparing to rain particles. Consequently, CPI probe [14] has been selected to conveniently calculate the physical sizes from crystal images which correspond to the crystal dimension and relating properties.

MATERIALS AND METHOD

The observation were conducted on 7 September 2011 over central Thailand within the geographical area bounded by 12N to 16N and 98E to 100.4E (Figure 1) in three provinces including (i) Suphan Buri (SB), (ii) Kanchanaburi (KC) and (iii) Ratchaburi (RC). The goal was to investigate the properties of tropical cirrus clouds and ice crystals. These data include four samples of cirrus clouds corresponding to 54.2 km of cloud penetration including two cirrostratus (Cs) and two Cirrus (Ci) with temperature between -8°C and 21°C at four different altitudes from 6 km to 10 km.

Airborne measurement and data sets consist of both cloud particle counter and imager instrument which were mounted on the Super King Air aircraft as exhibited in Figure 2. The instruments include Fast-FSSP, 2-DS and HVPS which measured particle number concentration and particle diameter at the size range from 0.47 to 19,200 μm. The aircraft is also equipped with a CPI probe for measuring the particle size and physical properties. Further information on these instrumentations is presented in Table 1.

The research aims to characterize the cloud microphysical properties including the total number concentration of cloud particles, particle number size distribution (hereafter referred to as PNSD), crystal dimensions, drop freezing and ice particle habits in tropical cirrus clouds. The measurements of these properties were taken during horizontal transects with Integrated airspeed (IAS) not exceeding 160 knots into the core of clouds where the high liquid water exists. The horizontal transects continued as far as safety allowed and then exited before penetrating the next cell in the higher altitude with ascending rate of around 500 ft/min. According to the specification of DRRAA's research aircraft, these flight observations are limited to the altitude of as high as 10 km.

Cloud Microphysical Measurement: Significant cloud microphysical measurements taken on 7 September 2011 over central Thailand are exhibited in Figure 3 with statistical data analysis shown in Table 2. These data were collected during two Cs and two Ci penetrations with the combined distance of 54.2 km. The measurements

Table 1: List of instrumentation on the research aircraft (KASET 2013) of DRRAA

Instrument	Purpose	Range
i) Fast-FSSP (Fast Forwarding Scattering Spectrometer Probe)	Cloud droplet spectra	0.47 to 50 mm
ii) 2-DS (Two Dimensional Spectrometer)	Cloud particle spectra	10 to 1,820 mm
iii) HVPS (High Volume Precipitation Spectrometer)	Precipitation spectra	150 to 19,200 mm
iv) CPI Probe (Cloud Particle Imager)	Cloud particles and ice crystal images	2.3 mm/pixel

Table 2: Statistics of cloud microphysical properties, particle sizes, and physical properties measured during the flight on 7 September 2011

Mission: Cloud types	Cloud 1: Cs (1)	Cloud 2: Cs (2)	Cloud 3: Ci (1)	Cloud 4: Ci (2)	Sum	Mean
Time (UTC)	07:44:12- 07:46:32	07:54:33-07:57:59	08:04:52-08:06:14	08:13:55-08:14:58		
Lat-Long	14.95857N, 99.32492E	13.83159N, 99.58006E	13.62263N, 99.59022E	13.3978N, 99.41677E		
Places	SB	KC	RC	RC		
Temperature (°C)	-8±0.6	-16±1.5	-20±0.5	-21±0.1		-16.25±0.7
Altitude (m)	6397±5.1	7866±197.2	8398±66.0	9266±21.5		7981.75±72.5
Total cloud length (km)	16.31	22.27	8.88	6.74	54.2	13.55
LWC (g/m^3)	0.34±0.18	0.45±0.26	0.35±0.13	0.07±0.05		0.30±0.2
Mean Updraft (m/s)	0.02	-2.99	-2.75	-1.09		-1.7
Minimum Updraft (m/s)	-4.3	-10.81	-2.03	-1.8		-4.74
Maximum Updraft (m/s)	3.88	18.74	-3.7	0.22		4.79
Mean diameter (μm)	13.2	80.5	27.8	281.6		100.78
GMD (D_g) (μm)	12.8	14.6	12.8	351		97.8
GSD (σ_g) (μm)	1.6	5.3	1.2	79.2		21.83
FSSP (#/L)	296.04±1461	2109.43±22429	2.01±13.45	0		602±5976
2-DS (#/L)	34927.29±39852	1370.03±2727	102.70±70.5	6.42±8.1		9102±10664
HVPS (#/L)	1.19±1.21	5.87±4.86	1.73±0.94	0.30±0.40		2.27±1.9
CPI Total count	5018	15620	9198	1397	31,233	7808.25
Mean D_L (μm)	62.7	77.7	80	56.9	69.325	69.33
Minimum D_L (μm)	3.25	3.3	3.3	3.3		3.29
Maximum D_L (μm)	1399.3	3012.6	3012.6	1053.7		2119.55
Mean D_w (μm)	43.2	52.1	56.7	40.4	48.1	48.1
Minimum D_w (μm)	2.3	2.3	2.3	2.3		2.3
Maximum D_w (μm)	1093.1	3010.1	3010.1	830.2		1985.88
Maximum value of AR	8.4	17.5	11	4.9	10.45	10.45
Fraction of spheroids particles : ice particles	17.46	6.83	6.86	6.96	8.45	9.53

All accepted particles are under the condition that "Length > 0 and Width > 0 and Area > 0" SB: Suphan Buri; KC: Kanchanaburi ; RC: Ratchaburi; GMD: Geometric standard deviation; GMD: Geometric mean diameter

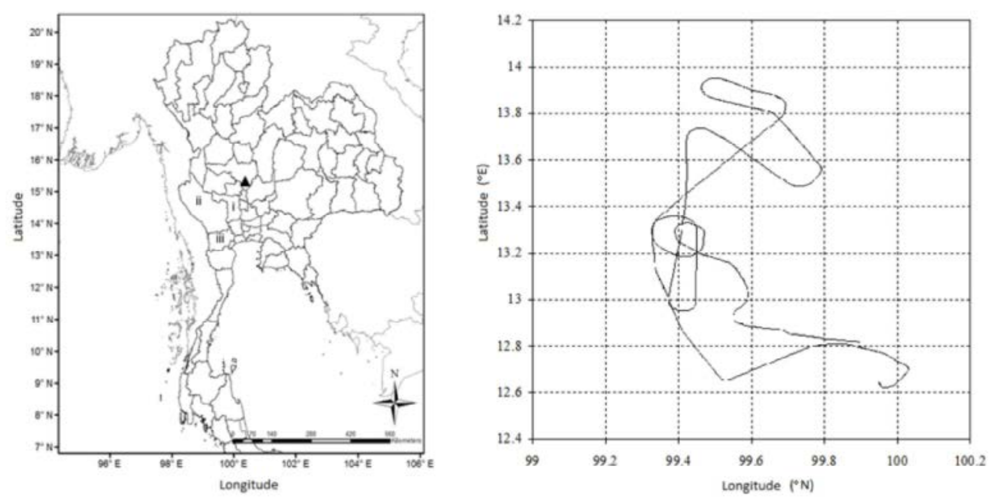

Fig. 1: (Left) The study area over central Thailand (the geographical area bounded by 12N to 16N and 98E to 100.4E) and the location of observational weather stations of DRRAA (triangles); (Right) Flight tracks through cirrus clouds in the central region of Thailand on 7 September 2011.

Fig. 2: The Super King Air aircraft (left) illustrating locations of Fast-FSSP and HVPS on the right wing (upper right), 2-DS and CPI Probe on the left wing (lower right).

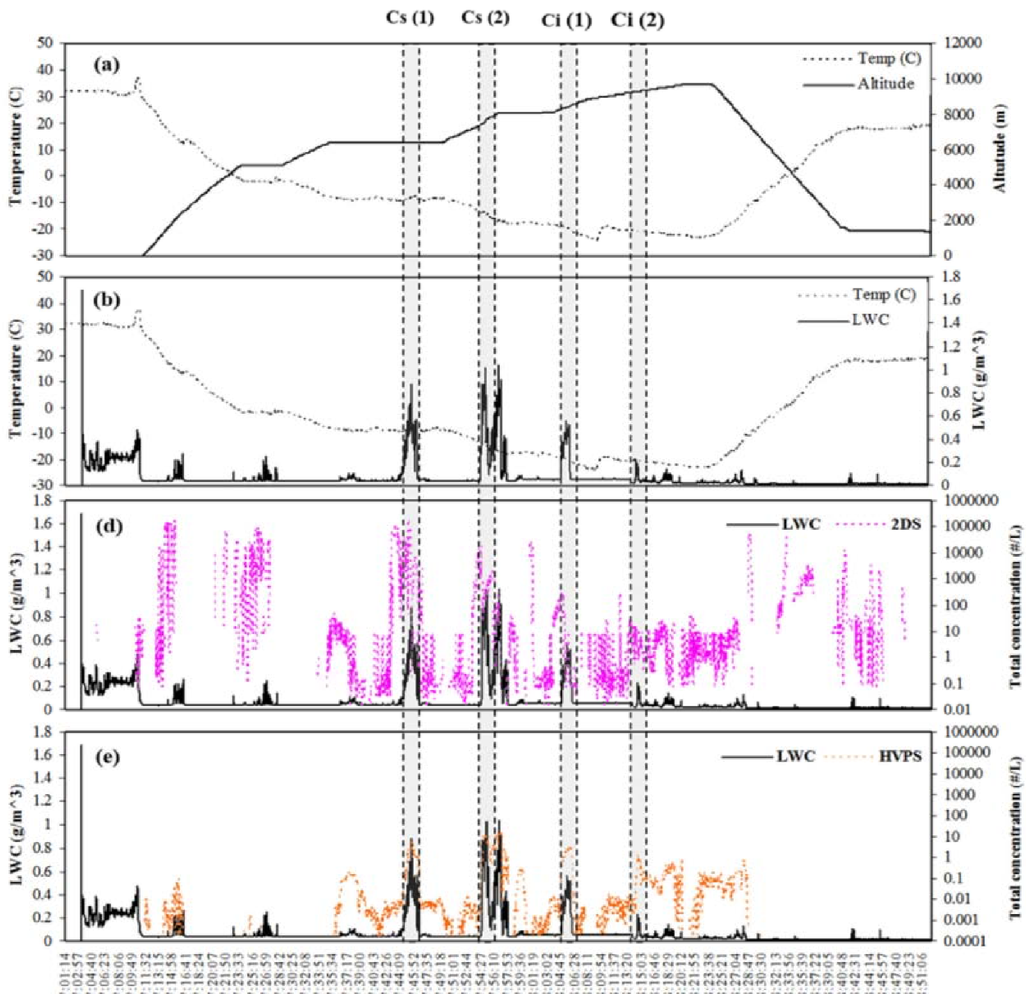

Fig. 3: Time history of (a) altitude and temperature (b) temperature and LWC (c) - (e) LWC with total number concentration from Fast-FSSP, 2DS and HVPS during the flight of the Super King Air on 07:01:14-08:51:06 UTC 7 September 2011.

Table 3: Weather condition on 7 September 2011 over central Thailand

NK station : 15° 15' 4.5" N, 100° 20" 13.87' at 0000UTC on the 7 September 2011											
KI	LI	TTI	SWI	SI	CAPE (J/kg)	Freezing level (m)	CCL (m)	Mean RH (at 20-25 kft) (%)	Wind speed (at 20-25 kft) (m/s)	Wind direction (at 20-25 kft) (degree)	Wind Shear SFC-6 km (m/s)
32.85	-0.3	40.9	231.2	1.22	98	4693.3	259.3	84	10.8	318	12.34

Fig. 4: Cirrus cloud sampled on 7 September 2011, selected cloud images: (a) - (b) Cirrostratus (Cs) and (c) - (d) Cirrus (Ci).

during the penetrations are shown in the highlighted area surrounded by dash lines. The images of the penetrated clouds are shown in Figure 4. The crucial cloud properties selected included altitude (m), temperature (°C), liquid water content (g/m^3), updraft velocity (m/s), total number concentration (#/L) and number concentration in each bin sizes from Fast-FSSP, 2DS and HVPS.

Ice Crystal Dimension and Physical Properties: A total of 31,233 CPI images of ice crystals from 7 September 2011 were used to analyze crystal dimensions and placed into crystal categories. The attributes include maximum particle image length (D_L), maximum width (D_W) that is transverse to the maximum length chord, projected area (A_{proj}), perimeter (P), focus value (i.e. how well the crystal is in focus), roundness and more sophisticated derivatives, such as radial harmonics (the Fourier transform of consecutive radii drawn from the particle centroid), see Table 2. Several of these attributes are used in conjunction to sort the particle images into ice crystal shape categories using the particle habit classification criteria as suggested by Lawson (2006) [14].

Meteorological Situation on 7 September 2011: Additional meteorological parameters for this study were observed by (1) the atmospheric observational stations of DRRAA and (2) HYSPLIT back trajectory modeling was used to collect the surface wind flow as shown in Figure 5.

During the observation on 7 September 2011, which is in wet season, the significant weather monitoring properties, instability indices and average surface wind flow over northern Thailand were measured as presented in Figure 5 and Table 3. The data support the following analysis.

- Almost all instability indices including KI, LI, TTI, SWI, SI and CAPE exhibited low convective potential or marginal instability.
- At high altitude, approximately between 20 and 25 kft, the high value of RH (> 80%) and moderate wind speed in the direction of north western were presented.
- The average surface wind flow directions from radiosonde continuously shifted from Southwest to

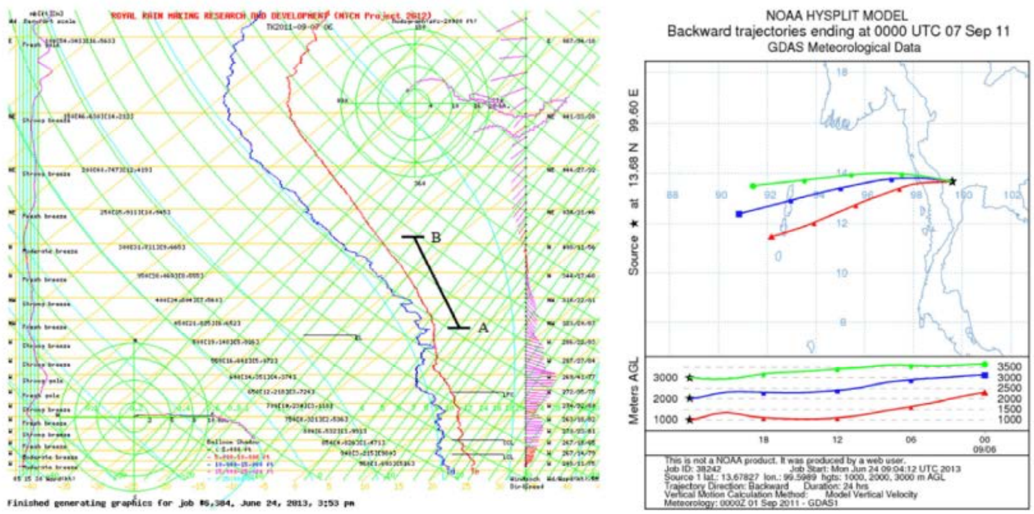

(a) (b)

Fig. 5: Additional meteorological parameters on 7 September 2011: (a) Skew-T plot diagram of a temperature (red) and dewpoint (blue), sounding taken at 0000UTC at central Thailand (NK station: 15O 15' 4.5" N, 100 O 20" 13.87') with A and B denote the interval of observational altitude base of the thin cirrus [15-16], (b) 24 hrs back-trajectory analysis from the NOAA HYSPLIT model. Plots were derived by READY website [17].

West with increasing altitude (surface to 3,000 m) from Andaman sea accord. The result from the HYSPLIT back trajectory modeling (24 hrs back trajectory at 1,000 - 3,000 m above ground) is illustrated in Figure 5(b).

RESULT AND DISCUSSION

Particle Number Size Distribution of Cirrus Clouds: The PNSD information was constructed by combining measurements from the FSSP, 2-DS and HVPS as shown in Figure 6. The width of bins and data channels were taken into account when the PNSD was computed in order to obtain the data which is independent of the measuring instruments [18]. Over the central Thailand on 7 September 2011, the observations show that the PNSD in each cloud is quite different with altitude above freezing level through allowable highest altitude (about 10 km). The differences are observed in four different levels from 6 km up to 10 km with two types of cirrus including Cs and Ci and temperatures ranged between 8°C and 21°C. Additional statistical data analysis is illustrated in Table 2.

It can be seen from the distribution of particle number concentration and size spectra in both cloud types that the geometric mean diameter (D_g) is reversely proportional to the temperature. In other words, the mean diameter tends to increase as the temperature lower. In the case of Cs, the D_g increases form 12.8 µm up to 14.6 µm as the temperature reduces from -8 °C to -16 °C. Similarly in Ci, the D_g changes from 12.8 µm up to 351.0 µm as the temperature decreases from -20 °C to -21 °C. Furthermore, the geometric standard deviation (σ_g) was tend to be higher than 1.2 [19]. The PNSD implies that these particles are almost polydisperse in cirrus clouds, which means that the particles in an ensemble have different sizes according to the measurement of CPI images.

Additionally from Figure 6, the observation shows that the total number concentration tends to gradually lower as the altitude increase and the temperature lower. The PNSD in Cs cloud clearly exhibited continuously wide size spectrum ranging from around 10 to 5500 µm. The maximum of large number concentration were found at 10 µm in both cases. On the other hands, the PNSD in Ci cloud exhibits a distribution close to a normal distribution. The spectrum is narrow with range around 10 to 4500 µm. Particle size at maximum number concentration found to be around 300 to 500 µm. Comparing to Cs clouds, Ci clouds particles were of larger diameters with lower total number concentration.

Measurement of Crystal Dimensions and Ice Particle Habits in Tropical Cirrus Cloud

Crystal Dimensions and Their Properties: The habit of the particles in the present study was characterized by

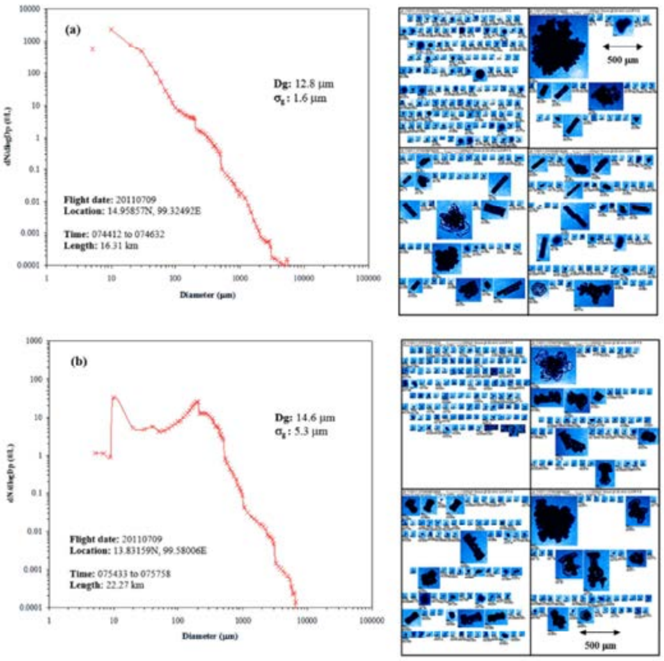

Fig. 6(a-b): The PNSD of tropical cirrus clouds arriving from the analysis of with Fast-FSSP, 2DS and HVPS data (left) and example of particle images from CPI (right); The data were collected during the flight of the Super King Air on 07:01:14-08:51:06 UTC 07 September 2011 at different temperatures and altitudes: (a) Cs (1), T = -8 oC, Alt = 6,397 m and (b) Cs (2), T = -16 oC, Alt = 7,866 m

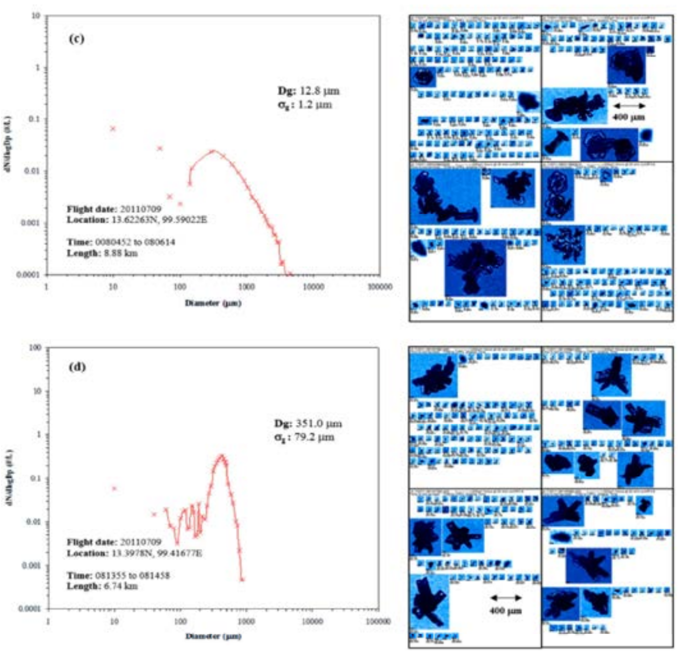

Fig. 6(c-d): The PNSD of tropical cirrus clouds arriving from the analysis of with Fast-FSSP, 2DS and HVPS data (left) and example of particle images from CPI (right); The data were collected during the flight of the Super King Air on 07:01:14-08:51:06 UTC 07 September 2011 at different temperatures and altitudes: (c) Ci (1), T = -20 oC, Alt = 8,398 m and (d) Ci (2), T = -21 oC, Alt = 9,266 m.

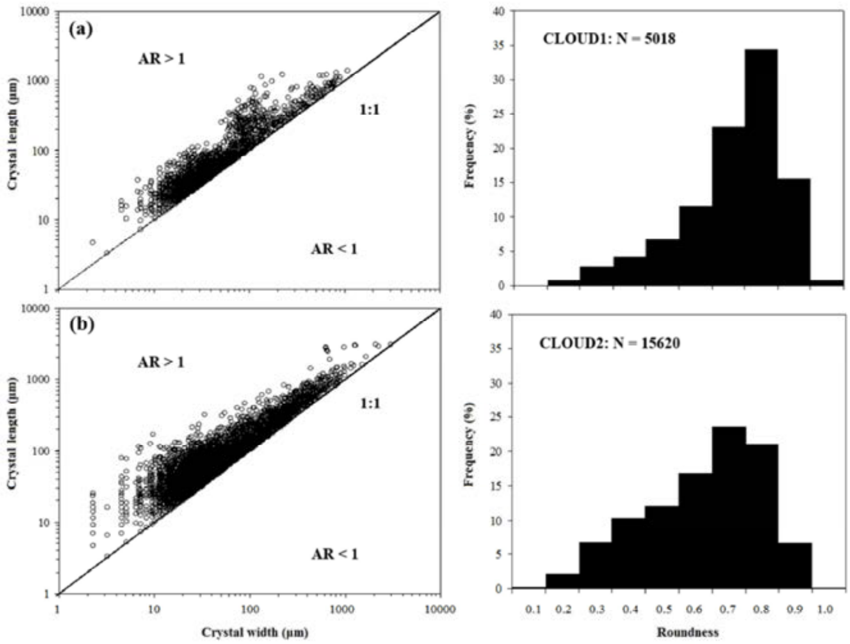

Fig. 7(1): Dimensions of AR (left): The dashed line with slope of 1 designates the boundary between AR < 1 and AR > 1; Distribution of RD in cirrus cloud (right): Images of theses crystals are shown in Fig. 6. The number in the upper right corner indicates sample as follows: (a) Suphan Buri, 07:44:12- 07:46:32 UTC, Cs, T = -8oC, Alt = 6397 m and (b) Kanchanaburi, 07:54:33-07:57:59 UTC, Cs, T = -16oC, Alt = 7866 m.

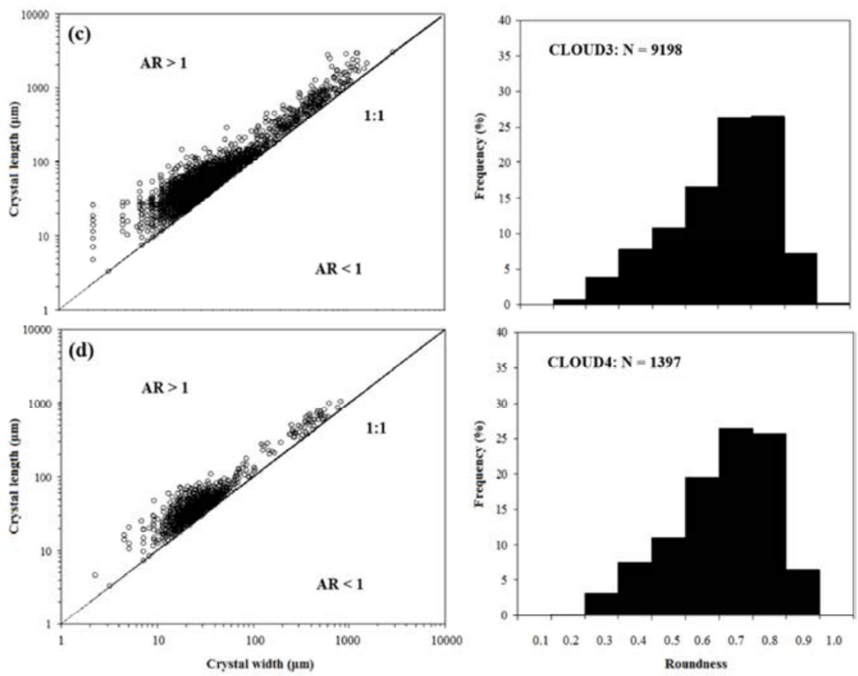

Fig. 7(2): Dimensions of AR (left): The dashed line with slope of 1 designates the boundary between AR < 1 and AR > 1; Distribution of RD in cirrus cloud (right): Images of theses crystals are shown in Fig. 6. The number in the upper right corner indicates sample as follows: (c) Ratchaburi, 08:04:52-08:06:14 UTC, Ci, T = -20oC, Alt = 8398 m and (d) Ratchaburi, 08:13:55-08:14:58 UTC, Ci, T = -21oC, Alt = 9266 m.

two dimensionless parameters referred to as aspect ratio (hereafter AR) and roundness (hereafter RD) [20]. The AR is a ratio between the crystal length and crystal width of the images. The RD can be considered as a measure of the circularity of the particle images with values vary from 0 to 1. It was assumed here that a circular shape implies a spherical particle. The crystal parameters included the crystal length (D_L), crystal width (D_w), RD, projection area, etc. These were extracted from raw CPI data by the CPIVIEW software developed by SPEC, Inc. The scatter plot of D_L versus D_w and the distribution of RD were illustrated in Figure 7.

The crystal with the maximum value of AR, between approximately 4.9 and 11, for the entire four cloud penetration of two cloud types with 31,233 total counts was shown in Table 2. The values of D_w for ice crystal range from 2.3 to 3010 µm with the averaged value for all cloud types of 48.1 µm. The values of D_L range from 3.25 to 3013 µm with the averaged value for all cloud types of 69.3 µm.

In cases of Cs clouds at altitude between 6 km and 8 km and temperature range of -8°C to -16°C with total length of penetration 38.6 km, the crystals show the maximum value of AR around 12.85. The values of D_w were in range of 3.25 to 3012.6 µm with the averaged value of 70.2 µm. The value of D_L falls between 2.3 and 3010.1 µm with the averaged value of 47.7 µm.

Also, in the event of Ci clouds at altitude between 8 km and 10 km and temperature range of -20°C to -21°C with total length of penetration 15.6 km, the crystals show the maximum value of AR around 7.95. The values of D_w were in range of 2.3 to 3010.1 µm and the averaged value of 48.6 µm. The value of D_L falls between 3.3 and 3012.6 µm with the averaged value of 68.5µm.

Fraction of Spherical Particles in Ice Clouds: The distributions of the AR and RD shown in Figure 7 can be considered as distortion functions and therefore be used for retrievals of the fraction of spherical images in measured distributions. Figure 8 shows an example of spherical particle images from CPI along the flight. Based on CPI View data extraction for crystal dimensions with the criteria of spherical particle classification as suggested by Lawson (2006) [14], the observation shows that the crystal length is less than or equal to 30 µm and the distribution of the RD for spherical particles results in the bin RD > 0.75 as illustrated in Figure 9. 5,643 crystal images were selected from all the cases. The images show that the fraction of spherical particles trends to increase with temperature when the temperature level is above -8°C (Case Cs(1)). As the temperature cools down between -16°C and -21°C the fraction of spheroids and ice particles become steady. The average ratio of spherical to ice particles for the four cloud passes is 8.45. These are summarized in Figure 9.

Crystal Habit Classification: During the total of 54.2 km cloud penetration on 7 September 2011, the temperature ranged from 8°C to 21°C. The CPI probe collected a total of 31,233 crystals images under the condition that D_L, D_w and A_{proj} exceed the predefined thresholds. The D_L threshold of 30 µm was chosen since the shape of smaller particles cannot be confidently categorized. As a result, the total of 5,643 crystal images were eliminated as exhibited in Figure 10. 25,590 crystals images are classified using acceptance criteria of Lawson (2006) [14] as long columns, thick plates and plates. These crystals are also called "diamond dust". The diamond dusts are typically observed under very thin, high clouds that are penetrated by the sun's rays and often produce optical effects such as halos and arcs. Other crystals are classified as bullet rosettes, budding rosettes, rosettes and complex with side planes. These types of crystals are also called "rosette shapes". Rosette shapes are polycrystals that are typically formed from rapid freezing of a super-cooled water drop or solution drop [21-22].

The habits of ice particles in cirrus clouds with D_L > 30 µm were categorized in three groups including rosette shapes, diamond dust and irregular. The overwhelming majority of ice particles (88%) were found to have an irregular shape and only 12% were rosette shapes (8.4%) and diamond dust (3.2%). Table 4 shows the percentage of crystal habit classification. The analysis of particle sizes and habits reveal that irregular shape particles are evenly distributed in all size categories, including small and large particles. However, the average size irregular in cirrus clouds trend to be a small ice particles of approximately 90 µm. The complex with side planes contribute the longest ice crystal in rosette shapes while the plate shapes illustrate the largest size in diamond dust.

In addition to the general classifications of diamond dust and rosette shapes, solid or hollow hexagonal prisms represent the majority of pristine ice in cirrus clouds diamond dusts (Figure 10) while the complex with side planes show the highest number for rosette shapes. As suggested in Table 4, the ice crystals in plate shapes and bullet rosettes are rare, which agrees with the finding

Table 4: The fraction of ice crystal habits in 4 sampled cirrus clouds observed by CPI

Cirrus	Diamond Dust						Rosette Shapes								Irregulars	
	Long columns		Thick plates		Plates		Bullet rosettes		Budding rosettes		Rosettes		Complex crystals		Irregulars	
	FRA (%)	MD_L (μm)	FRA (%)	MD_L (μm)	FRA (%)	MD_L (μm)	FRA (%)	MD_L (μm)	FRA (%)	MD_L (μm)	FRA (%)	MD_L (μm)	FRA (%)	MD_L (μm)	FRA (%)	MD_L (μm)
Cs (1)	4.41	226.20	0.74	99.17	0.26	172.72	0.68	416.88	2.48	70.84	2.76	254.79	4.92	379.07	83.75	90.10
Cs (2)	2.53	107.17	0.49	112.23	0.28	246.96	0.11	322.57	3.50	53.71	0.97	232.35	4.48	420.76	87.65	94.99
Mean Cs	**3.47**	**166.69**	**0.62**	**105.70**	**0.27**	**209.84**	**0.40**	**369.73**	**2.99**	**62.28**	**1.87**	**243.57**	**4.70**	**399.92**	**85.70**	**92.55**
Ci (1)	1.46	68.23	0.46	65.80	0.15	223.29	0.05	378.52	2.77	49.20	0.38	308.98	3.11	308.98	91.61	97.99
Ci (2)	1.50	77.64	0.71	80.23	0.00	N/A	0.00	N/A	2.12	46.68	0.26	553.40	5.03	519.79	90.39	68.94
Mean Ci	**1.48**	**72.94**	**0.59**	**73.02**	**0.08**	**223.29**	**0.03**	**378.52**	**2.45**	**47.94**	**0.32**	**431.19**	**4.07**	**414.39**	**91.00**	**83.47**
Mean All	**2.48**	**119.81**	**0.60**	**89.36**	**0.17**	**214.32**	**0.21**	**372.66**	**2.72**	**55.11**	**1.09**	**337.38**	**4.39**	**407.15**	**88.35**	**88.01**

*FRA is the fraction in percentage of total crystals and MD_L is mean MD_L in μm

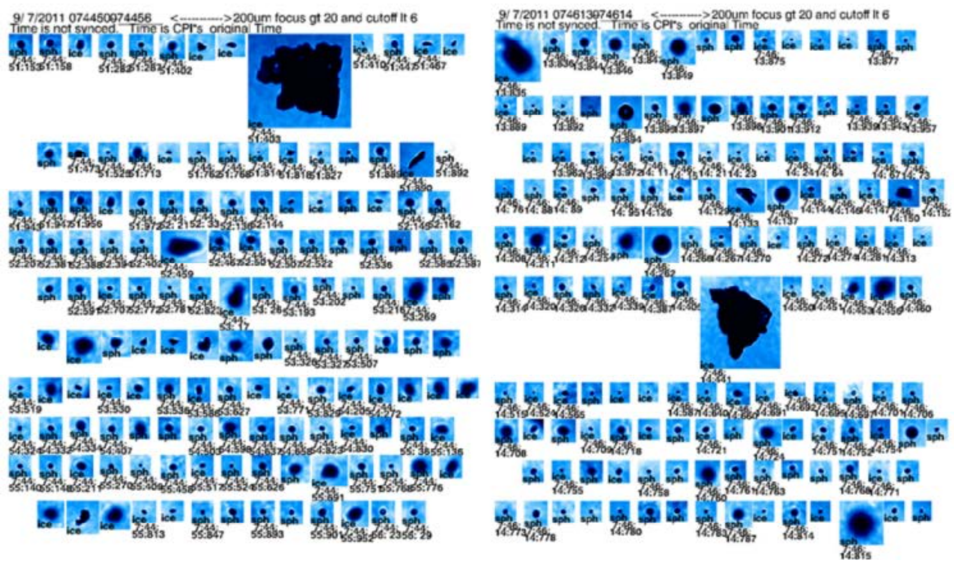

Fig. 8: Spherical particle images from CPI along the flight.

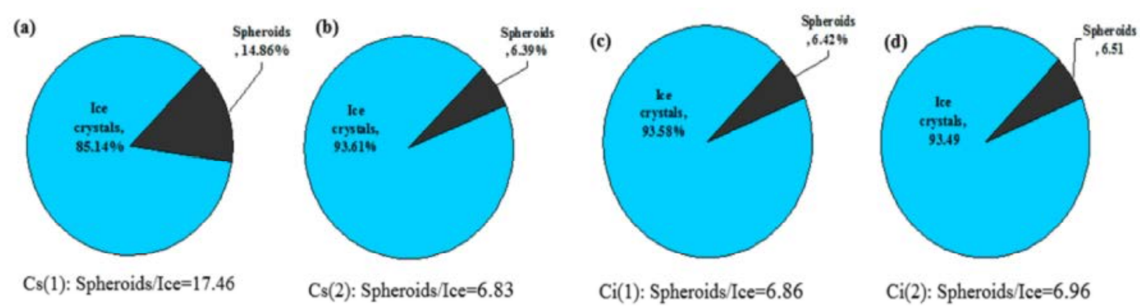

Fig. 9: The frequency (fraction) of classified spherical particles in cirrus clouds (left) for 4 cases on 7 September 2011: (a) Cs (1): Suphan Buri, 07:44:12- 07:46:32 UTC, T = -8oC, Alt = 6397 m. (b) Cs (2): Kanchanaburi, 07:54:33-07:57:59 UTC, T = -16oC, Alt = 7866 m. (c) Ci (1): Ratchaburi, 08:04:52-08:06:14 UTC, T = -20oC, Alt = 8398 m. (d) Ci (2): Ratchaburi, 08:13:55-08:14:58 UTC, T = -21oC, Alt = 9266 m and (e) an example of spherical particle images from CPI along the flight.

in Korolev (1999) [23]. The ratio of diamond dust, rosette shapes and irregular shapes was found to be proximately 1: 3: 35 on average over all observed cirrus.

The habits of irregular ice particles observed can generally be categorized into two different types according to Korolev as follows [23]. The first type is faceted polycrystalline consisting of combinations of

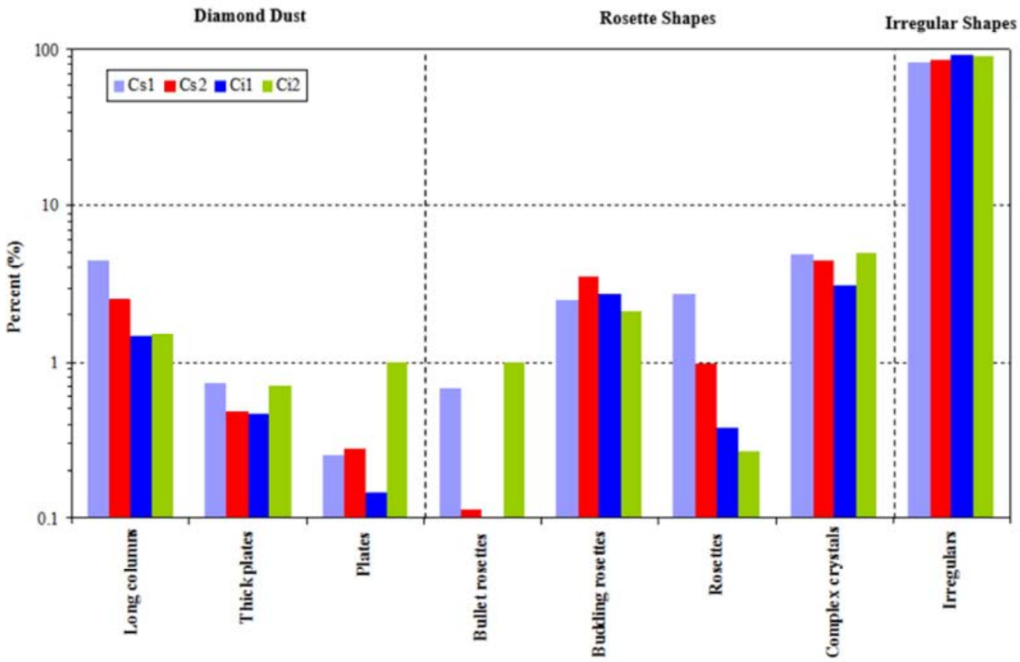

Fig. 10: The diagram shows the percentage of number of ice crystal habits observed by CPI during all the cloud penetrations on 7 September 2011 for each habit categories. Long columns, thick plates, and plates are associated with diamond dust. Bullet rosettes, budding rosettes, rosettes, and complex with side planes are associates with rosette shapes. Small irregular and large irregular are associates with irregular shapes. The total number of ice crystals categorized is 25,590.

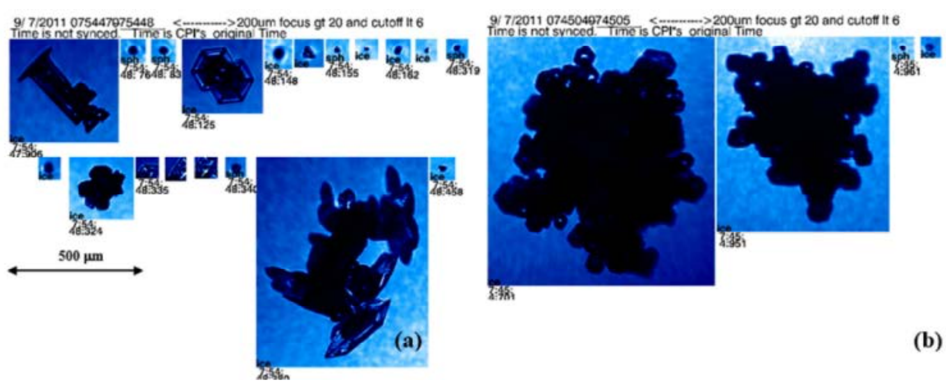

Fig. 11: Examples of the habits of irregular ice particles in cirrus clouds over Central Thailand on 7 September 2011 from -8oC to -21oC, with cloud height ranging from 6 km to 10 km: (a) faceted polycrystalline particles and (b) shapeless ice particles.

different habit ice crystals such as plates, columns, etc. growing in different directions (Figure 11a). The second type is ice particles with smooth curving sides and edges. These types of particles frequently have potato-like shapes indicating that these particles are the result of sublimation (solid to vapor) (Figure 11b) [24].

CONCLUSIONS

The Results Obtained Were as Followed:

- The PNSD in Cs clouds clearly exhibit continuously wider size spectrum with higher total number concentration than Ci cloud. On the other hand, Ci clouds exhibit larger particle diameters with dominated size around 300 to 500 μm, the mode particle size in Cs clouds were proximately 10 μm.

- The averaged maximum AR of all sampled cirrus cloud particles ranges between 4.9 and 11. Cs clouds evidently illustrate a larger AR than Ci clouds.
- The fraction of spherical particles of size range less than 30 μm in cirrus clouds is proximately 8.45%. In this study, when the temperature is less than -16°C, the ratio of spheroids to ice particles in both cirrus types are similar. The ratios tend to be stable toward cooler temperatures.
- It appears that the cirrus clouds in this study are mostly formed from irregular ice crystals, where the pristine ice crystals are rare. The analysis of particle sizes and habits showed that irregular shape particles are evenly distributed in all size categories and usually trend to be small ice particles of approximately 90 μm. It is highly probable that a similar conclusion will be reached for mid latitude and Arctic clouds [23].

The information about the habits of ice particles obtained here gives an insight into the mechanisms of ice formation in clouds. This suggests that as the results, the ice crystals of irregular shape particles will have different radiative characteristics than used in climate model parameterizations. They will also grow at different rates than pristine ice. Therefore, it is necessary that more extensive characterization of the habits of atmospheric ice particles be made in different regions and associations with different cloud types.

However, the observations of this study is only limited to one day. The results may not be representative of the entire wet season in Thailand. Indeed, the subject of cirrus clouds and climate in Thailand is a challenging problem in the atmospheric and climate sciences and requires considerable observational and theoretical research and development.

ACKNOWLEDGEMENTS

The authors gratefully acknowledge the Department of Royal Rainmaking and Agricultural Aviation (DRRAA), Bangkok Thailand, for funding support through the 2012 Aerosol and CCN in Thailand Research Project. We appreciate the Research Group for providing the data sets of cloud particles. We would like to also thank the Royal-Rainmaking's Atmospheric Observation Group for weather observation data used in this study.

REFERENCES

1. Liou, K.K., 1986. Influence of cirrus clouds on weather and climate processes: A global perspective, Mon. Wea. Rev., 114: 1167-1198.
2. Dowling, D.R. and F.L. Radke, 1990. A summary of the Physical Properties of Cirrus Clouds. Journal of Applied Meteorology, 29: 970-978.
3. Sauvage, L., H.F. Pierre, C. Hélène, B. Gérard, T. Vincent, P. Jacques and A. Franck, 1999. Remote Sensing of Cirrus Radiative Parameters during EUCREX'94. Case Study of 17 April 1994. Part I: Observations. Mon. Wea. Rev., 127: 486-503.
4. Garrett, T.J., H. Gerber, D.G. Baumgardner, C.H. Twohy, D.G. Baumgardner and E.M. Weinstock, 2003. Small, highly reflective ice crystals in low-latitude cirrus, Geophys. Res. Lett., pp: 30, doi:10.1029/2003GL018153.
5. Heymsfield, A.J., C.G. Schmitt, A. Bansemer, D. Baumgardner, E.M. Weinstock, J.T. Smith and D. Sayres, 2004. Effective ice particle densities for cold anvil cirrus, Geophys. Res. Lett., pp: 31, doi:10.1029/2003GL018311.
6. Jensen, E., D. Starr and O.B. Toon, 2004. Mission investigates tropical cirrus clouds, EOS, 85: 45-50.
7. Wendisch, M., P. Pilewskie, J. Pommier, S. Howard, P. Yang, A.J. Heymsfeld, C.G. Schmitt, D. Baumgardner and B. Mayer, 2004. Impact of cirrus crystal shape on solar spectral irradiance: A case study for subtropical cirrus, J. Geophys. Res., pp: 110, doi:10.1029/2004JD005294.
8. Baran, A.J., S.J. Brown, J.S. Foot and D.L. Mitchell, 1999. Retrieval of Tropical Cirrus Thermal Optical Depth, Crystal Size and Shape Using a Dual-View Instrument at 3.7 and 10.8.m. J. Atmos. Sci., 56: 92-110.
9. Heymsfield, A.J. and G.M. McFarquhar, 1996. High Albedos of Cirrus in the Tropical Pacific Warm Pool: Microphysical Interpretations from CEPEX and from Kwajalein, Marshall Islands. J. Atmos. Sci., 53: 2424-2451.
10. McFarquhar, G.M. and A.J. Heymsfield, 1997. Parameterization of Tropical Cirrus Ice Crystal Size Distributions and Implications for Radiative Transfer: Results from CEPEX. J. Atmos. Sci., 54: 2187-2200.

11. McFarquhar, G.M. and A.J. Heymsfield, 1998. The Definition and Significance of an Effective Radius for Ice Clouds. J. Atmos. Sci., 55: 2039-2052.
12. McFarquhar, G.M., A.J. Heymsfield, J. Spinhirne and B. Hart, 2000. Thin and Subvisual Tropopause Tropical Cirrus: Observations and Radiative Impacts. J. Atmos. Sci., 57: 1841-1853.
13. Dye, J.E. and D. Baumgardner, 1984. Evaluation of the forward scattering spectrometer probe: I. Electronic and optical studies. J. Atmos. Ocean. Tech., 1: 329-344.
14. Lawson, R.P., A.B. Brad, Z. Patrick, O.C. Daren and M. Qixu, 2006. Microphysical and Optical Properties of Atmospheric Ice Crystals at South Pole Station. Journal of applied Meteorology and Climatology. 45: 1505-1524.
15. Garrett, T.J., B.C. Navarro, C.H. Twohy, E.J. Jensen, D.G. Baumgardner, P.T. Bui, H. Gerber, R.L. Herman, A.J. Heymsfield, P. Lawson, P. Minnis, L. Nguyen, M. Poellot, S.K. Pope, F.P.J. Valero and E.M. Weinstock, 2005. Evolution of a Florida Cirrus Anvil. Journal of the Atmospheric Sciences. 62: 2352-2372.
16. Knollenberg, R.G., K. Kelly and J.C. Wilson, 1993. Measurement High Number Densities of Ice Crystals in the Tops of Tropical Cumulonimbus. Journal of Geographical Research. 98: 8693-8664.
17. Rolph, G.D., 2011. Real-time Environmental Applications and Display sYstem (READY) Website (http://ready.arl.noaa.gov). NOAA Air Resources Laboratory, Silver Spring, MD.
18. Hobbs, P.V. and A.L. Rangno, 1985. Ice Particle Concentrations in Clouds. Journal of the Atmospheric Sciences. 42: 2523-2549.
19. Kulkami, P., P.A. Baron and K. Willeke, 2011. Aerosol Measurement: Principles, Techniques and Applications, Third et. John Wiley & Son, Inc.
20. Korolev, A. and G. Isaac, 2003. Roundness and Aspect Ratio of Particles in Ice Clouds. Journal of the Atmospheric Sciences. 60: 1796-1808.
21. Bacon, N.J., M.B. Baker and B.D. Swanson, 2003. Initial stages in the morphological evolution of vapour-grown ice crystals: A laboratory investigation. Quart. J. Roy. Meteor. Soc., 129: 1903-1927.
22. Pruppacher, H.R. and J.D. Klett, 1997. Microphysics of Clouds and Precipitation. 2d ed. D. Reidel, pp: 954.
23. Korolev, A.V., G.A. Isaac and J. Hallett, 1999. Ice particle habits in Arctic clouds. Geophys. Res. Lett., 26: 1299-1302.
24. Orltay, R.G. and J. Hallett, 1989. Evaporation and melting of ice crystals: A laboratory study, Atmos. Research, 24: 169-189.